

A dressed-bag model study of the final-state $N\Delta$ interaction in pion-photoproduction processes off the deuteron

I.T. Obukhovskiy and V.I. Kukulin

Institute of Nuclear Physics, Moscow State University, 119899 Moscow, Russia

Murat M. Kaskulov* and Peter Grabmayr†

Physikalisches Institut, Universität Tübingen, D-72076 Tübingen, Germany

Amand Faessler

Institut für Theoretische Physik, Universität Tübingen, D-72076 Tübingen, Germany

(Dated: November 5, 2018)

The impact of the short-range $N\Delta$ interaction on the pion photoproduction processes off the deuteron in the Δ -resonance region is studied in the framework of recently proposed dressed-bag model. A common dressing procedure for bare three- and six-quark states is used to describe both the pion decay widths of baryon resonances and the effective NN (or $N\Delta$) interaction at short ranges related to the inner dressed-bag states. It is shown that the effect of short-range $N\Delta$ interaction for the forward-angle π^0 photoproduction off the deuteron cannot be neglected. The prospects for further development of the model to describe the short-range NN (or $N\Delta$) correlations in the lightest nuclei are discussed.

PACS numbers: 13.40.Gp, 12.39.Jh

I. INTRODUCTION

The Δ -isobar degrees of freedom play a crucial role in the description of numerous processes in nuclear and hadron physics. In such a description the Δ -isobar is either generated in the process itself or can be considered as “preexisting” in the wave function of the initial system. In any case we need to understand the dynamics for the Δ -isobar in a nuclear system, which in turn requires the construction of an adequate model for the $N\Delta$ interaction. The long-range part of the $N\Delta$ interaction is governed by the π -exchange, but its intermediate- and short-range parts are poorly known up to date, and thus it is an important topic for further studies. On the other hand, at low energies the Δ -isobar due to its rather high mass should be taken in the far off-shell region, and thus, the short-range part of the $N\Delta$ interaction will be essential for the understanding of many low- and intermediate-energy processes.

Unfortunately, even for the NN system which has been studied in much more details than the $N\Delta$ system the short-range part of the interaction is known rather poorly. In the current NN models the short-range part of the interaction (e.g. the high-momentum behaviour of vertex form factors in the meson-exchange models) is only fitted to the experimental NN phase shifts. Because such a fit would be hardly possible for the $N\Delta$ system, one should resort to a consistent microscopic treatment of the short-range interaction within a realistic model with a common set of parameters for the NN and $N\Delta$ systems. In our opinion any consistent microscopic treatment of short-range NN and $N\Delta$ interactions should include both quark and meson degrees of freedom.

The quark approach to the short-range NN interaction has a more than two-decade history during which many methods have been developed, e.g. the adiabatic [1, 2, 3, 4] and resonating group methods (RGM) [5, 6], quark compound bag (QCB) model [8, 9], hybrid models [10], etc. These models are in agreement with the NN data at intermediate energies, but all of them treat the inner NN -system on a rather phenomenological level. Important meson field degrees of freedom remain absent.

In the recently proposed Moscow-Tübingen dressed-bag model [11] we start from the quark-configuration analysis of the RGM wave function including the configuration mixing at short range [12] and take into consideration the proper meson cloud including 2π and σ contributions of the bag-like six-quark component in the overlap region around 0.6 fm. Contrary to other models which exploit the meson cloud coupled to the quark core of the nucleon (e.g. the cloudy bag model [13]) we have formulated our approach to the six-quark intermediate states using the Fock-column representation for the vectors of state and we have proposed a new mechanism for the dressing of the six-quark bag

*Electronic address: kaskulov@pit.physik.uni-tuebingen.de

†Electronic address: grabmayr@uni-tuebingen.de

with the σ -meson field. With three phenomenological parameters in each partial wave L the model describes the NN scattering data for $L \leq 2$ up to 1 GeV with high precision including the tensor mixing and all the properties of the deuteron [11]. We assume that the model describes the short-range $N\Delta$ interaction as well. In both channels, NN and $N\Delta$, the short-range interaction is determined by the same constraint originating from the Pauli exclusion principle.

Another key problem in this field is the possibility of tests of this part of the $N\Delta$ interaction. If one samples the $N\Delta$ wave function by quasielastic (e, e') knock-out of the Δ -isobar (or of the nucleon) from the deuteron, it would be rather a study of a “preexisting” $N\Delta$ component. Another method consists in the Δ -isobar excitation by real photons and in a study of the off-shell $N\Delta$ rescattering amplitude in the final state (diagram in Fig. 1(a)). We have selected the pion photoproduction reactions $d(\gamma, \pi^0 pn)$ and $d(\gamma, \pi^- pp)$ in the Δ -resonance region in a kinematic setting which maximises the pion kinetic energy. The corresponding forward-angle photoproduction cross sections are sensitive to the short-range part of the $N\Delta$ interaction. To prove this statement we evaluate the contribution of the short-range $N\Delta$ final-state interaction (FSI) to the pion photoproduction cross section starting from the constituent quark model (CQM) for baryons and from the dressed-bag model [11] for NN and $N\Delta$ interactions.

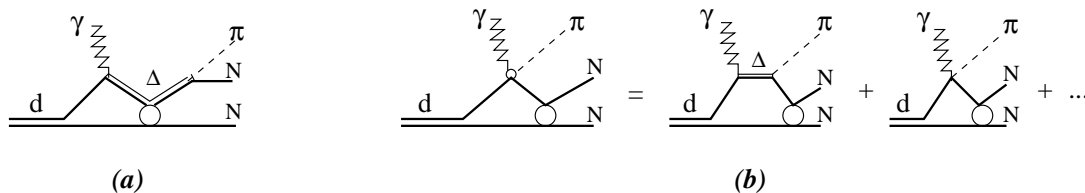


FIG. 1: Loop diagrams of FSI for the “direct” short-range $N-\Delta$ interaction before the pion emission (a) and for the NN rescattering after the pion emission (b)

The CQM describes with reasonable accuracy all the electro-magnetic and strong production processes at least for the free nucleon [14, 15, 16]. The results for free nucleons can readily be generalized for any baryon and for the six-quark component of any nucleon-baryon system. Here we consider π photoproduction in the Δ -resonance region, but such a consideration could be easily extended to η photoproduction in the S_{11} -resonance region, or to other similar cases. Even though the CQM approach is limited in use by a non-relativistic harmonic-oscillator (h.o.) basis and a naive 3P_0 model of meson production, there is the advantage, that it allows us to embody all the relevant baryon resonances in the reaction mechanism with predictable amplitudes. The corresponding experimental data can be directly related to the internal structure of these resonances.

Up to now the role of the $N\Delta$ final state interaction (FSI) in the pion photoproduction off nuclei has been poorly investigated. We recall that the Δ -resonance region at $E_\gamma \approx 250$ -350 MeV is most convenient for such a study since the influence of other resonances, e.g. $P_{11}(1440)$ or $S_{11}(1535)$, is negligible in this region, and thus the main mechanism of photoproduction is a quasifree process with a virtual Δ -isobar excitation. It is well known that the contribution of this mechanism to the π^0 production off the deuteron overestimates the forward-angle cross section [17, 18, 19] by a factor of 1.5 to 2 and that the FSI should play a decisive role in this region [20]. Recent evaluations [21] have shown that taking into account the pn FSI can bring theoretical predictions into better agreement with the data [22].

It is quite plausible that the $N\Delta$ FSI plays also a certain role in the π^0 photoproduction along with the NN FSI [21], and if so, there will be a possibility to study the $N\Delta$ interaction in the photoproduction processes on nuclei. The contribution of the direct $N\Delta$ interaction to pion production depends essentially on the off-shell behaviour of the $N\Delta$ amplitude because of the integration over the inner momenta in the loop diagram shown in Fig. 1(a).

Earlier attempts to take the direct $N\Delta$ interaction into account in terms of an s -channel resonance pole mechanism [17] did not bring a detectable improvement in the description of the data. On the other hand there is a successful coupled-channel ($NN + N\Delta$) approach to pion production in NN collisions [23], and for the full study of the FSI problem it would be desirable to include a couple-channel description of both NN and $N\Delta$ final states. Then the long-distance $N\Delta$ correlations would be fully taken into consideration.

In a more simple approach, which is used here, the final-state NN interaction includes diagrams with $N\Delta$ intermediate states, as shown in Fig. 1(b) by the diagrammatic representation of this interaction. The virtual $N\Delta$ channel is partially taken into account in the NN FSI. Simplifying the problem in such a manner, we imply further that the diagram in Fig. 1(a) is related only to the “direct” short-range $N\Delta$ interaction.

By the following prescriptions of the dressed-bag model we evaluate here the contribution of this “direct” short-range $N\Delta$ FSI to the differential cross section and show that this contribution is not small and cannot be neglected. As a first step of the study, it is demonstrated by comparison of the results of two simplified models for pion photoproduction off the deuteron: (i) the quasifree mechanism, (ii) the quasifree mechanism modified by the $N\Delta$ FSI Born term. A more realistic variation of the model considering both NN and $N\Delta$ half-off-shell t-matrices in the FSI loop integrals

is in progress.

In Sect. II of this paper, the quark-configuration analysis of NN and $N\Delta$ systems in the overlap region is briefly reviewed, and the constraints following from the Pauli exclusion principle are formulated. The effective short-range $N\Delta$ interaction is deduced from the dressed-bag model with the same method as for the NN interaction in Ref. [11]. In Sect. III, pion photoproduction off the nucleon in the Δ -resonance region is described in terms of the CQM. The dressing of a bare (three-quark) Δ -isobar and other baryons is carried out with the 3P_0 model. On this basis the ‘‘off-shell’’ Δ propagator is obtained. In Sect. IV, the results on pion photoproduction off the deuteron are discussed and the concluding remarks are given in Sect. V.

II. SHORT-RANGE $N\Delta$ INTERACTION

Within the quark-model the short-range $N\Delta$ and NN interactions are very similar to each other. In fact, in the lowest partial waves, in the even ($L = 0, 2$) and in the odd ($L = 1, 3$) states, quark configurations of the NN and $N\Delta$ overlap have the same structure determined by the constraint following from the Pauli exclusion principle. We consider here only the lowest even partial wave $L = 0$ for the spin-isospin state $ST = 10$ in the NN channel and for $ST = 11$ and $ST = 21$ in the $N\Delta$ channel. These quantum numbers are important for the pion photoproduction off the deuteron in the Δ -resonance region.

A. Configuration mixing in NN and $N\Delta$ overlap regions

Microscopic evaluations [12] made in the RGM approach lead to the following picture of configuration mixing in the overlap region as depicted in Fig. 2. In both $NN(ST=10)$ and $N\Delta(ST=21)$ channels the overlap can be described by a

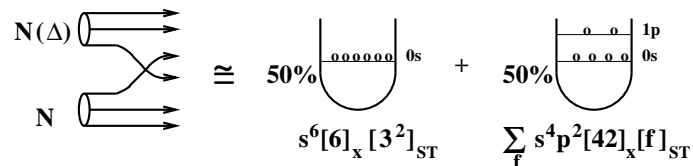


FIG. 2: Configuration mixing at short range in the $NN(ST=10)$ (or $N\Delta(ST=21)$) channel.

fully symmetric configuration $s^6 [6]_x$ which has a probability of $\approx 50\%$ in the overlap region $r \lesssim 0.6-1$ fm; the other 50% being a superposition of states in $2\hbar\omega$ -excited configurations s^4p^2 , which are characterized by a non-trivial coordinate Young tableaux $[42]_x$. However, in the other $N\Delta$ channel ($ST=11$) the fully symmetric state s^6 is forbidden by the Pauli exclusion principle.

The states in 6q-configurations s^6 and s^4p^2 differ in their inner structure:

- (i) The fully symmetric configuration s^6 is a bag-like state with its charge-spin structure strictly constrained by the Pauli exclusion principle. In both channels, $NN(ST=10)$ and $N\Delta(ST=21)$, the Young tableaux in the product of spin and isospin spaces $[3^2]_{ST}$ is fixed by the condition to be conjugate to the colour Young tableau $[2^3]_C$. The fully antisymmetric state $[1^6]_{CST}$ can only be constructed as an inner product of mutually conjugate states $[2^3]_C \circ [3^2]_{ST}$.
- (ii) In the excited six-quark shell-model states s^4p^2 of $[42]_x$ and $[6]_x$ symmetry, the non-trivial coordinate Young tableau $[42]_x$ allows all the possible tableaux $[f_{ST}]$ in the inner product of spin and isospin spaces for both $NN(ST=10)$ and $N\Delta(ST=21)$ channels:

$$\begin{aligned} NN(10) : \quad [f_{ST}^{(N)}] &= [42]_S \circ [3^2]_T = [51]_{ST} + [3^2]_{ST} + [41^2]_{ST} + [321]_{ST} + [2^2 1^2]_{ST}, \\ N\Delta(21) : \quad [f_{ST}^{(\Delta)}] &= [51]_S \circ [42]_T = [51]_{ST} + [42]_{ST} + [3^2]_{ST} + [41^2]_{ST} + [321]_{ST}. \end{aligned} \quad (1)$$

(This is also true for the other $N\Delta$ channel $ST=11$ which contains the product $[42]_S \circ [42]_T$).

Consequently, in the configuration s^4p^2 in each ST channel there is a six-dimensional basis with vectors labelled by a set of Young tableaux $f = \{[f_x], [f_{ST}]\}$, where $[f_x] = [6], [42]$ and $[f_{ST}]$ takes all the values $[f_{ST}^{(N)}]$ or $[f_{ST}^{(\Delta)}]$ from Eq.(1):

$$\begin{aligned} d_f(s^4p^2) &= |s^4p^2 [f_x] [f_{ST}^{(N)}](ST=10), L=0\rangle \quad \text{and} \\ D_f(s^4p^2) &= |s^4p^2 [f_x] [f_{ST}^{(\Delta)}](ST=21), L=0\rangle, \end{aligned} \quad (2)$$

where d_f and D_f are the excited quark-shell-model configurations with the NN and $N\Delta$ quantum numbers respectively. This is a sufficiently large basis to represent the main features of the NN or $N\Delta$ channels at short ranges. In Ref. [12] it was also shown that some linear combinations of the basis states (Eq.2) are genuine NN (or $N\Delta$) cluster-like states, which can be referred to as the short-range wave functions $\{\Psi_{NN}\}_{sr}$ and $\{\Psi_{N\Delta}\}_{sr}$

$$\begin{aligned}\{\Psi_{NN}\}_{sr} &= \sum_f C_f^{(N)} d_f(s^4 p^2) = \mathcal{A} \{\varphi_{2S}(r) N(1, 2, 3) N(4, 5, 6)\} \quad \text{and} \\ \{\Psi_{N\Delta}\}_{sr} &= \sum_f C_f^{(\Delta)} D_f(s^4 p^2) = \mathcal{A} \{\varphi_{2S}(r) N(1, 2, 3) \Delta(4, 5, 6)\},\end{aligned}\quad (3)$$

where \mathcal{A} is the antisymmetrizer $\mathcal{A} = \frac{1}{10}(I - \sum_{i=1}^3 \sum_{j=4}^6 P_{ij})$ and $N(1, 2, 3)$ and $\Delta(4, 5, 6)$ are the nucleon and Δ -isobar states with fixed numbers of quarks $i(j)$. The coefficients $C_f^{(N)}$ and $C_f^{(\Delta)}$ are algebraic ones apart from a common energy-dependent factor (which can be calculated in principle by solving the RGM equations, see e.g. Ref. [12]). It is particularly remarkable that these cluster-like states correspond to a nodal wave function $\varphi_{2S}(r)$ which describe the relative motion of two clusters with $\mathbf{r} = \frac{1}{3}(\mathbf{r}_1 + \mathbf{r}_2 + \mathbf{r}_3 - \mathbf{r}_4 - \mathbf{r}_5 - \mathbf{r}_6)$ as the relative coordinate. In the present case it is the $2S$ state of the h.o. basis $\varphi_{2S}(r) \sim (1 - r^2/b^2) e^{-3r^2/4b^2}$, but in general it would be a more realistic nodal wave function. Here b is the h.o. radius, which is a scale parameter with a typical value of $b \approx 0.5-0.6$ fm.

Such a decomposition of the total antisymmetrized short-range NN ($N\Delta$) wave function into two mutually orthogonal parts:

(i) a non-nucleonic (bag-like) state

$$\begin{aligned}d_0(s^6) &= |s^6[6]_X [3^2]_{ST} (ST = 10), L=0\rangle \quad (\text{for the } NN \text{ overlap}), \\ D_0(s^6) &= |s^6[6]_X [3^2]_{ST} (ST = 21), L=0\rangle \quad (\text{for the } N\Delta \text{ overlap}),\end{aligned}\quad (4)$$

and (ii) a ‘‘proper’’ NN (or $N\Delta$) component [Eq. (3) with $f \neq 0$], is characteristic of any quark-model approach. This property is independent on the choice of the quark-quark interaction. It is a specific manifestation of the Pauli exclusion principle in the system of six colored quarks. It is interesting that in the $ST = 11$ $N\Delta$ channel a symmetric bag-like state s^6 of Eq. (4)-type is forbidden, and thus the complete wave function of the $N\Delta$ system at short ranges in that channel reduces to a net nodal cluster-like state of Eq. (3)-type. In a general case the NN or $N\Delta$ wave function should be written as a two-component Fock column.

To be precise, the representation (Eq.3) of the cluster wave function $\Psi_{NN}(r)$ or $\Psi_{N\Delta}(r)$ is only meaningful in the region $0 \leq r \lesssim b \div 2b$. The full wave function of the system has a two-channel structure, namely the two-component Fock column:

$$\begin{pmatrix} \Psi_{NN} \\ d_0(s^6) + \text{cloud} \end{pmatrix} \quad \text{or} \quad \begin{pmatrix} \Psi_{N\Delta} \\ D_0(s^6) + \text{cloud} \end{pmatrix},\quad (5)$$

In Fig. 3, the ‘‘cloud’’ is represented by the σ -meson s -channel loop.

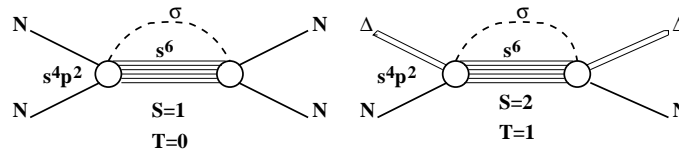


FIG. 3: Loop diagram contributions to the short-range NN and $N\Delta$ interaction.

A similar picture can also be observed in the lowest odd partial wave, i.e. $L = 1$, where the configuration $s^5 p[51]_X$ has a trivial symmetry $[51]_X$ in coordinate space and its spin-isospin wave function is strictly constrained by the Pauli exclusion principle. The corresponding bag-like state in the channel $ST = 11$

$$d_1(s^5 p) = |s^5 p[51]_X [321]_{ST} (S_1 T_1 = 11), L_1=1\rangle \quad (6)$$

is also contributing to the considered processes. At the same time, in the excited configuration $s^3 p^3[3^2]_X$ the ‘‘true’’ cluster-like NN (or $N\Delta$) states are allowed, and a corresponding cluster wave function $\varphi_{3P}(r)$ has also a node at short ranges.

However, for the total angular momentum $J^P = 2^+$ of the initial $N\Delta$ state a full set of possible $d_1 + \pi$ intermediate states with the total isospin $T = 1$ includes 11 shell-model configurations $d_1(s^5 p)$ with different values of the spin $S_1 = 1, 2, 3$ (in the simplest case of the S -wave pion), the isospin $T_1 = 0, 1, 2$ and the Young tableaux $[f_{ST}] = [321], [42]$. The configuration (6) is only an example of the basis vector from this set.

B. Dressed-bag model

It has been proposed [11], that the non-nucleonic bag-like states $s^6[6]_x$ and $s^5p[51]_x$ with trivial coordinate symmetry in two lowest partial waves $L = 0$ and 1, respectively, (in NN and $N\Delta$ channels), acquire their own meson clouds which are different from the sum of two meson clouds of the initial baryons. Probably, such a cloud will serve to stabilize the six-quark bag in the NN (or $N\Delta$) overlap region. For example, it looks tempting to consider the scalar-isoscalar (σ -meson) field as most strong in the presence of the six-quark bag. The quark masses are reduced in the scalar field, and such a “dressed” bag (see Fig. 3) should be much lower in energy than the corresponding six-quark shell-model states s^6 (s^5p).

Thus we come to the following dynamical model [11] which can be tested in numerous processes:

- (i) At short ranges there is an enhanced σ -field originating from transitions between the “proper” NN cluster-like state $\{\Psi_{NN}\}_{sr}$ and the bag-like one $d_0(s^6)$

$$\{\Psi_{NN}\}_{sr} \leftrightarrow d_0 + \sigma \quad (7)$$

- (ii) The short-range NN dynamics is determined by coupled-channel equations for the two channels of Eq. (7).
- (iii) An effective separable and energy-dependent NN potential $V_{NqN}(r, r'; E)$ emerges after exclusion of the closed channel $d_0 + \sigma$ by use of standard methods [24] of nuclear physics. This potential is related to the corresponding s -channel loop diagram (see Fig. 3), the contribution of which to the short-range NN force can be calculated in terms of the 3P_0 model (see Ref. [11]).

The effective potential for the short-range $N\Delta$ interaction is determined by the same scheme of calculations. Since the method has been described in Ref. [11] we sketch here only the basic outline of the calculation.

We start from the Hamiltonian for quark-pion coupling deduced from the 3P_0 model [15] in the form that takes into account the Galilean invariance for the system of n constituent quarks ($n=3$ or 6, see numbering in Fig. 4) with equal masses $m_q = m_N/3$ (see the details in Refs. [11, 25, 26]),

$$H_{\pi qq}^{(n)}(\mathbf{k}, \lambda) = -i \frac{f_{\pi qq}}{m_\pi} \tau_{-\lambda} e^{i \frac{n-1}{n} \mathbf{k} \cdot \boldsymbol{\rho}} O(\boldsymbol{\rho}, \boldsymbol{\rho}') \boldsymbol{\sigma} \cdot \left[\frac{\omega_\pi}{2m_q} \left(\frac{2}{i} \nabla_\rho + \frac{n-1}{n} \mathbf{k} \right) + \left(1 + \frac{\omega_\pi}{2nm_q} \right) \mathbf{k} \right] \quad \text{and} \\ O(\boldsymbol{\rho}, \boldsymbol{\rho}') = e^{-i \frac{1}{2} \mathbf{k} \cdot (\boldsymbol{\rho} - \boldsymbol{\rho}')} \Psi_\pi(\boldsymbol{\rho} - \boldsymbol{\rho}'), \quad (8)$$

written here in relative coordinates of the n -th quark $\boldsymbol{\rho} = \frac{1}{n-1} \sum_{i=1}^{n-1} \mathbf{r}_i - \mathbf{r}_n$. It is coincident with a local pseudo-vector (PV) coupling (taken in a non-relativistic approximation), when the pion radius b_π approaches zero (Fig. 4)

$$\Psi_\pi(\boldsymbol{\rho} - \boldsymbol{\rho}') \rightarrow \delta(\boldsymbol{\rho} - \boldsymbol{\rho}') \quad \text{for} \quad b_\pi \rightarrow 0. \quad (9)$$

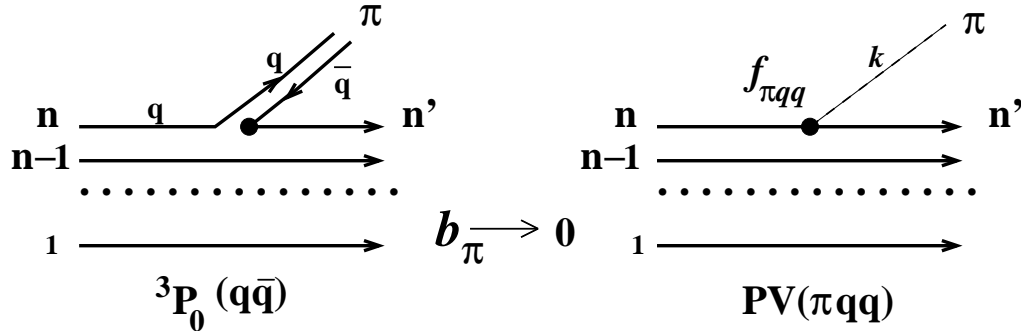


FIG. 4: Quark-pion coupling in the n -quark system.

The σ -meson is considered as a broad resonance ($\Gamma_\sigma \approx m_\sigma \approx 500$ MeV) in the π - π system with a simple vertex function

$$v_{\pi\pi\sigma}(\mathbf{k}, \mathbf{k}') \equiv \langle \sigma(\mathbf{k} + \mathbf{k}') | H_{\sigma\pi\pi} | \pi(\mathbf{k}) \pi(\mathbf{k}') \rangle = g_{\pi\pi\sigma} F_{\pi\pi\sigma}(q^2) \quad (10)$$

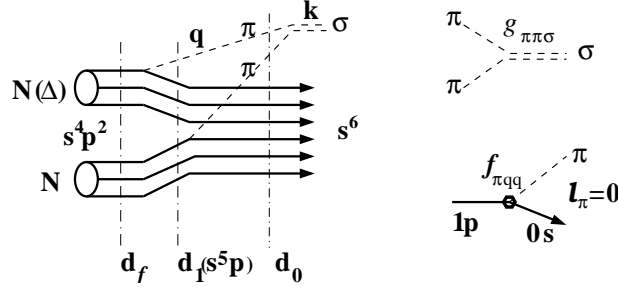


FIG. 5: Triangle loop diagram of σ -meson emission and its vertices.

with $\mathbf{q} = (\mathbf{k} - \mathbf{k}')/2$ and with a Gaussian form factor $F_{\pi\pi\sigma}(q^2) = e^{-q^2 b_\sigma^2/2}$ and a standard value $g_{\pi\pi\sigma} \approx 2-4$ GeV [27]. The σ is emitted from the cluster-like configuration $s^4 p^2$ in transition to the bag-like s^6 through two subsequent pion emissions with the de-excitation of p-shell quarks $d_f(s^4 p^2) \rightarrow d_1(s^5 p) \rightarrow d_0(s^6)$ (or $D_f(s^4 p^2) \rightarrow D_1(s^5 p) \rightarrow D_0(s^6)$) as is shown in Fig. 5.

Starting from the representation (3) of a short-range NN (or $N\Delta$) wave function, the $NN \rightarrow d_0 + \sigma$ (or $N\Delta \rightarrow D_0 + \sigma$) vertex function $\Gamma_{N\sigma q}$ (or $\Gamma_{\Delta\sigma q}$) can be written in the form

$$\Gamma_{N\sigma q}(k, E) = \sum_f C_f^{(N)} \Gamma_f^{(N)}(k, E), \quad \Gamma_{\Delta\sigma q}(k, E) = \sum_f C_f^{(\Delta)} \Gamma_f^{(\Delta)}(k, E), \quad (11)$$

where the partial vertices $\Gamma_f^{(N, \Delta)}(k, E)$ are quark-shell-model matrix elements for the transitions $d_f \rightarrow d_0 + \sigma$ ($D_f \rightarrow D_0 + \sigma$) shown in Fig. 5:

$$\Gamma_f^{(N)}(k, E) = 15 \times \sum_\lambda (1\lambda 1 - \lambda|00) \sum_{d_1} \int d^3 q \quad \langle \sigma(\mathbf{k}) | H_{\sigma\pi\pi} | \pi(\mathbf{q}) \pi(\mathbf{q} - \mathbf{k}) \rangle \frac{1}{E - H_{2\pi+d_0}} \\ \times \langle d_0 | H_{\pi qq}^{(5)}(\mathbf{q} - \mathbf{k}, -\lambda) | d_1 \rangle \frac{1}{E - H_{\pi+d_1}} \langle d_1 | H_{\pi qq}^{(6)}(\mathbf{q}, \lambda) | d_f \rangle. \quad (12)$$

Here $H_{2\pi+d_0}$ and $H_{\pi+d_1}$ are undisturbed energies of the intermediate states $2\pi + d_0$ and $\pi + d_1$ of the transitions

$$H_{\pi+d_1} = m_{d_0} + \frac{k^2}{2m_{d_0}} + \omega_\pi(\mathbf{q}) + \omega_\pi(\mathbf{q} - \mathbf{k}) \quad \text{and} \quad H_{\pi+d_1} = m_{d_1} + \frac{k^2}{2m_{d_1}} + \omega_\pi(\mathbf{q}) \quad (13)$$

with $m_{d_0} \approx m_{d_1} \approx 2300-2500$ MeV as a phenomenological parameter. In Eq. (12) the sum over d_1 includes all the 11 $d_1(s^5 p)$ configurations listed after Eq. (6) in the previous Subsection.

The spin- and isospin-flip matrix elements of the operators defined in Eq. (8) for 5-th and 6-th quarks $\langle d_0 | H_{\pi qq}^{(5)}(\mathbf{q} - \mathbf{k}, -\lambda) | d_1 \rangle$ and $\langle d_1 | H_{\pi qq}^{(6)}(\mathbf{q}, \lambda) | d_f \rangle$ are calculated in the limit of Eq. (9) with the standard fractional parentage coefficients (f.p.c.) technique of the quark shell model (see refs. [2, 3, 11, 25] for details). The results for NN [11] and $N\Delta$ channels are similar to each other:

$$\Gamma_{N\sigma q}(k, E) = \frac{f_{\pi qq}^2}{m_\pi^2} \frac{g_{\sigma\pi\pi}}{m_q^2 b^3} C_{ST}^N \mathcal{D}(k, E) \quad \text{and} \quad \Gamma_{\Delta\sigma q}(k, E) = \frac{f_{\pi qq}^2}{m_\pi^2} \frac{g_{\sigma\pi\pi}}{m_q^2 b^3} C_{ST}^\Delta \mathcal{D}(k, E). \quad (14)$$

Here only the algebraic factors $C_{10}^N = \frac{-19}{486} \sqrt{\frac{5}{3}}$ and $C_{21}^\Delta = \frac{113}{3645} \sqrt{\frac{5}{6}}$ are different for NN and $N\Delta$ channels because of different spin-isospin quantum numbers $ST = 10$ and 21 . Hence the effective ‘‘coupling constants’’ for transitions of Eq. (7) can be defined in a simple form dependent on fixed parameters of the model (πqq and $\sigma\pi\pi$ constants, masses m_π , m_σ , h.o. radius b) and an algebraic factor depending on the ST values

$$g_{N\sigma q} = g_{\sigma q N} = \frac{f_{\pi qq}^2}{m_\pi^2} \frac{g_{\sigma\pi\pi}}{m_q^2 b^3} C_{ST}^N \quad \text{and} \quad g_{\Delta\sigma q} = g_{\sigma q \Delta} = \frac{f_{\pi qq}^2}{m_\pi^2} \frac{g_{\sigma\pi\pi}}{m_q^2 b^3} C_{ST}^\Delta \quad (15)$$

However, the ‘‘form factor’’ $\mathcal{D}(k, E)$ (common for both above channels as well) has a more uncertain magnitude since it is obtained by the integration over the inner momenta q of the triangle loop diagram (Fig. 5), and thus

it depends on the generally unknown high-momentum behaviour of the πqq and $\sigma\pi\pi$ form factors. After a simple modification of each CQM Gaussian in the form

$$e^{-\alpha^2 q^2} \rightarrow e_{mod}(-\alpha^2 q^2) = (1-p)e^{-\alpha^2 q^2} + p e^{-\alpha^2 q^2/z^2}, \text{ with } p = \frac{1}{3} \text{ and } z \approx 2, \quad (16)$$

which does not dramatically change the low-momentum behaviour of all the CQM form factors, but enhances its high-momentum component by modifying the h.o. scale $b \rightarrow b/z$ [36], the contribution of the diagram in Fig. 6 to the σNN coupling leads to a realistic value $g_{\sigma NN}$. It should be noted that in contrast to a simple version proposed in Ref. [28] our calculations imply the summation over all possible three-quark intermediate configurations up to 2 h.o. quanta.

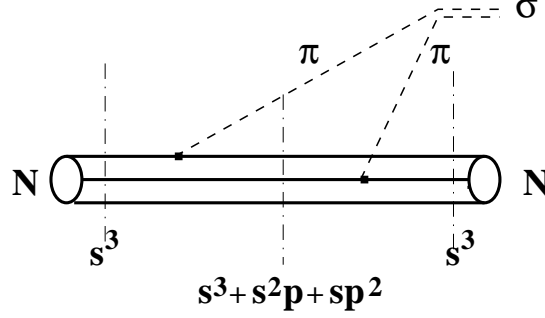


FIG. 6: Triangle loop diagram for the σ -nucleon coupling constant $g_{\sigma NN}$.

C. Reduction to effective non-local NN and $N\Delta$ interactions

The s -channel loop diagram in Fig. 3 with vertices calculated in the previous subsection (see Fig. 7) can be reduced

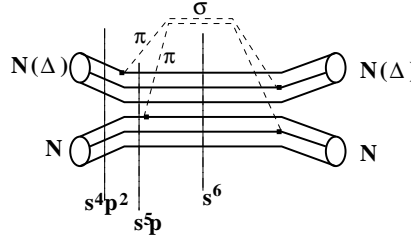


FIG. 7: The s -channel loop diagram of NN ($N\Delta$) interaction.

to a non-local attractive NN (or $N\Delta$) interaction potential of the form

$$V_{NqN}(r, r'; E) = \int d^3 k \varphi_{2s}(r') \Gamma_{N\sigma q}(k, E) \frac{1}{E - H_{\sigma+d_0}} \Gamma_{q\sigma N}(k, E) \varphi_{2s}(r) \quad (17)$$

After integration over the inner momentum \mathbf{k} the following expressions for effective NN and $N\Delta$ potentials arise

$$V_{NqN}(r, r'; E) = g_{N\sigma q}^2 I(E) |\varphi_{2s}(r')\rangle \langle \varphi_{2s}(r)| \quad \text{and} \quad V_{\Delta q \Delta}(r, r'; E) = g_{\Delta\sigma q}^2 I(E) |\varphi_{2s}(r')\rangle \langle \varphi_{2s}(r)|, \quad (18)$$

where the energy-dependent function $I(E)$ is common for both potentials

$$I(E) = \int d^3 k \frac{\mathcal{D}(k, E)^2}{E - H_{\sigma+d_0}} \quad (19)$$

Note that such a factorization of $V_{NqN}(r, r'; E)$ and $V_{\Delta q \Delta}(r, r'; E)$ into an ‘‘algebraic part’’ (constants $g_{N\sigma q}^2$ and $g_{\Delta\sigma q}^2$) and a common for both channels integral part $I(E)$ is characteristic of the dressed-bag model.

The significance of this effective interaction is two-fold:

(i) it projects the short-range NN (or $N\Delta$) wave function onto the nodal $2S$ state through the projection operator

$$\hat{P}_{2S} = |\varphi_{2S}(r')\rangle\langle\varphi_{2S}(r)|, \quad (20)$$

which determines a specific form of the short-range correlations (e.g. these correlations are seen in the NN scattering as a “repulsive-core-like” behaviour of the S-wave phase shift [11]);

(ii) it emphasizes the Pauli exclusion principle which imposes the restriction not only on the form but also on the relative strength [$g_{N\sigma q}$ and $g_{\Delta\sigma q}$ in Eq. (15)] of the short-range interaction in each ST channel.

To gain a better understanding of the proposed mechanism for the short-range interaction an analytical (Pade-) approximation for the integral in Eq. (19) as a function of energy E has been performed in Ref. [11]. An accurate approximation for $I(E)$ exhibits a pole behaviour

$$I(E) \approx \lambda_0 \frac{E_0 - a_0 E}{E_0 - E}, \quad (21)$$

with E_0 close to the mass of the primitive state $s^6 + \sigma$. The value of a_0 is too small ($a_0 \approx 0.05$) to lead to a detectable modification of the pole behaviour of Eq. (21). But the value λ_0 calculated with the same set of parameters as it was used in the above calculation of the coupling constant $g_{\sigma NN}$ turns out too small to give a realistic description of the NN phase shifts. We found that a considerable renormalization of λ_0 (factor 2 to 4) is necessary [11] to obtain a good description for the NN phase shifts up to 1 GeV. However, the considered mechanism is qualitatively correct.

The quantitative description is also possible [11] by fitting the values λ_0 , E_0 and a_0 as free parameters in order to describe the NN phase shift. In such a procedure the NN interaction through meson exchange is also considered for long ranges $r \gtrsim b$. The following parameters for the short-range NN interaction were obtained [11]:

$$g_{N\sigma q}^2 \lambda_0 = 328.55 \text{ MeV}, \quad E_0 - 2m_N = 693 \text{ MeV} \quad a_0 = -0.05 \quad \text{and} \quad b = 0.5065 \text{ fm} \quad (22)$$

which are used in the present work to describe the $N\Delta$ short-range interaction in the $ST = 21$ channel with the substitution $g_{N\sigma q} \rightarrow g_{\Delta\sigma q}$. Such substitution implies that effective coupling constant $g_{N\sigma q}$ should be roughly reduced in 1.7 times for $N\Delta$ interaction, and the effective parameter λ_0 in the separable potential (18)-(21) should be roughly reduced in three times. But such evaluations of the interaction on the basis of algebraic factors in Eq. (14) are only reliable to the order of magnitude, and thus our calculations of the effect of $N\Delta$ FSI have been performed for the reduced and non-reduced value of the constant λ_0 (see Sect. IV).

D. The $N\Delta$ and “dibaryon” mechanisms of pion emission from the deuteron

In the π^0 and π^- photoproduction off the deuteron there are at least two different mechanisms of pion emission shown in Figs. 8 and 9. In both cases there is the same intermediate $N\Delta$ state in the 5S_2 partial wave generated

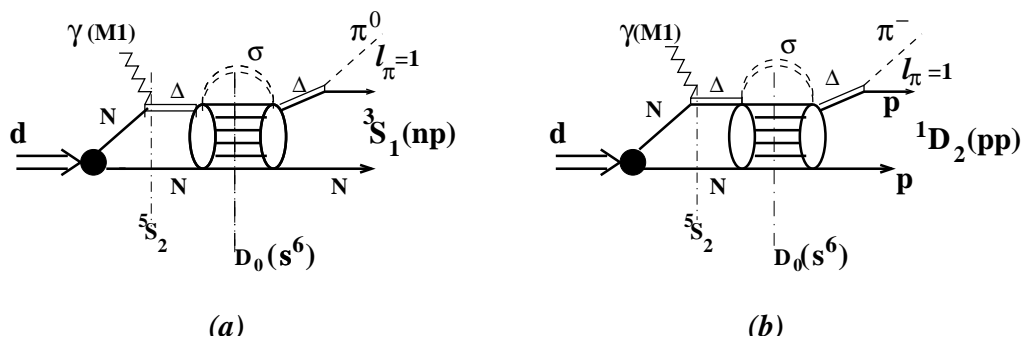


FIG. 8: The FSI of $N\Delta$ type with a P -wave pion.

by the isovector $M1$ $\gamma N \rightarrow \Delta$ transition on one of the nucleons. Note that for the other $N\Delta$ partial wave 3S_1 the analogous bag-like component $D_0(s^6)$ with $ST = 11$ is forbidden. However the final $\pi^0 pn$ and $\pi^- pp$ states are different in isospin of the NN subsystem. As a result the lowest partial wave 3S_1 in the np final state is allowed, but in the

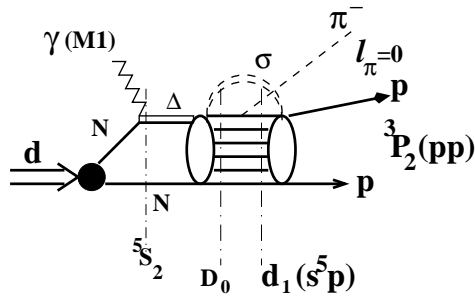


FIG. 9: The FSI of “dibaryon” type with the S -wave pion.

final pp state ($T=1$) the lowest 1S_0 wave is forbidden. The $^1D_2(pp)$ partial wave is only allowed through mechanisms shown in Fig. 8(b).

However, the $D_0(s^6)$ bag-like state with $ST = 21$ can bypass the transition to the final $^5S_2(N\Delta)$ state allowing the direct transition to the final $\pi^- pp$ state with a $^3P_2(pp)$ partial wave with the S -wave pion, as it is shown in Fig. 9. In this case the P -wave bag-like state $d_1(s^5p)$ of Eq. (6) is produced after the S -wave π^0 emission instead of the even-parity final state $^1D_2(pp)$ produced by P -wave π^- emission. Hence the dressed bag $d_1(s^5p) + \sigma$ should contribute to the π^- emission and could be seen as a correlated pp pair in the $^3P_2 - ^3F_2$ partial waves. Such a correlated pp pair has to absorb the recoil pion momentum as a whole. A possible dibaryon resonance with the quantum numbers of $d_1(s^5p) + \sigma$ system could enhance the role of such a correlated pp pair, and thus any polarization experiments which will be able to make a selection of the final pp pair in the $^3P_2 - ^3F_2$ states would be desirable.

But in general (i.e. without the dibaryon enhancement) the role of $N\Delta$ FSI interaction in the π^- photoproduction should be considerably smaller than in the π^0 case. In Sect. IV this qualitative analysis will be supported by quantitative evaluations made in the framework of the CQM.

III. PION PHOTOPRODUCTION OFF THE NUCLEON

First we want to test our approach in pion photoproduction from free nucleons. These processes are enhanced in the resonance region by the excitation of virtual baryons. In the CQM, as a rule, we deal with bare (i.e. three-quark) baryons which can be treated as h.o. 3q configurations in the translationally-invariant shell model (TISM)

$$\begin{aligned}
 N(940) &= |s^3[3]_{XL} = 0\rangle_{TISM} \cdot |[1^3]_C[3]_{ST} S = 1/2, T = 1/2\rangle, \\
 \Delta(1232) &= |s^3[3]_{XL} = 0\rangle_{TISM} \cdot |[1^3]_C[3]_{ST} S = 3/2, T = 3/2\rangle, \\
 R(1440) &= |sp^2[3]_{XL} = 0\rangle_{TISM} \cdot |[1^3]_C[3]_{ST} S = 1/2, T = 1/2\rangle \quad \text{and} \\
 N^*(1535) &= |s^2p[21]_{XL} = 1\rangle_{TISM} \cdot |[1^3]_C[3]_{ST} S = 1/2, T = 1/2\rangle
 \end{aligned} \tag{23}$$

with a simple structure of the coordinate part, e.g.

$$|s^3[3]_{XL} = 0\rangle_{TISM} = \varphi_{0S}(\rho_1/\alpha_1)\varphi_{0S}(\rho_2/\alpha_2), \tag{24}$$

$$|sp^2[3]_{XL} = 0\rangle_{TISM} = \sqrt{\frac{1}{2}}[\varphi_{0S}(\rho_1/\alpha_1)\varphi_{2S}(\rho_2/\alpha_2) + \varphi_{2S}(\rho_1/\alpha_1)\varphi_{0S}(\rho_2/\alpha_2)], \dots, \text{etc.}, \tag{25}$$

where the h.o. basis wave functions

$$\varphi_{0S}\left(\frac{\rho}{\alpha}\right) = (\pi\alpha^2)^{-3/4}e^{-\rho^2/2\alpha^2}, \quad \varphi_{1P}^m\left(\frac{\rho}{\alpha}\right) = (\pi\alpha^2)^{-3/4}\sqrt{\frac{2}{3}}\frac{\rho}{\alpha}e^{-\rho^2/2\alpha^2}\sqrt{4\pi}Y_{1m}(\hat{\rho}), \dots, \text{etc.} \tag{26}$$

depend only on the relative quark coordinates $\rho_1 = \mathbf{r}_1 - \mathbf{r}_2$, $\rho_2 = (\mathbf{r}_1 + \mathbf{r}_2)/2 - \mathbf{r}_3$, $\alpha_1 = \sqrt{2}b$, $\alpha_2 = \sqrt{3/2}b$.

The most important ingredient of any model for photoproduction is the procedure for the dressing of the bare baryons by meson fields. Here we consider a procedure starting from the 3P_0 model [15, 25, 26].

A. Dressing of bare baryons and the off-shell Δ propagator

The bare baryons should be dressed by the pion field to acquire finite decay widths. Then, for example, the Δ isobar acquires a finite decay width $\Gamma_\Delta \approx 120$ MeV, but the nucleon remains stable. For simplicity all the calculations are

performed with the undressed w.f. for the nucleon, but for the Δ -isobar a standard dressing procedure (see, e.g. [29]) based on a self-energy loop diagram contribution to the mass of Δ (see diagram in Fig. 10) has been performed:

$$\Sigma_{\Delta}(E) = \sum_{\lambda} \int \frac{d^3k}{(2\pi)^3 2\omega_{\pi}} \frac{v_{\Delta}^{\dagger}(\mathbf{k}, \lambda) v_{\Delta}(\mathbf{k}, \lambda)}{E - M_N - k^2/2M_N - \omega_{\pi}(k) + i0} \quad (27)$$

The $\pi N \Delta$ vertex function $v_{\Delta}(\mathbf{k}, \lambda)$ in Eq. (27), where \mathbf{k} is a (relative) momentum of the pion π^{λ} , $\lambda = 0, \pm 1$ in the

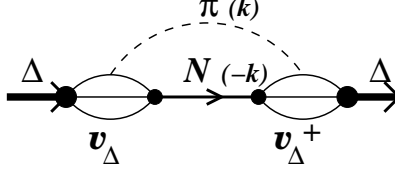


FIG. 10: Dressing of the Δ -isobar.

πN system, has been calculated within the CQM using the 3P_0 model as a matrix element of the operator Eq.(8) for the transition $\Delta \rightarrow \pi N$ in the limit of Eq.(9).

$$v_{\Delta}(\mathbf{k}, \lambda) = 3 \langle N(\mu_N, t_N) | H_{\pi qq}^{(3)}(\mathbf{k}, \lambda) | \Delta(\mu_{\Delta}, t_{\Delta}) \rangle = i \left(\frac{2\sqrt{2} f_{\pi qq}}{m_{\pi}} \right) e^{-k^2 b^2/6} \mathbf{S} \cdot \mathbf{k} T_{\lambda}, \quad (28)$$

In Eq. (28) the transition operators $S_m(T_{\lambda})$ are components of the total spin (isospin) of the $3q$ system in the spherical basis. Their matrix elements related to the spin (isospin) Clebsch-Gordan coefficients through the standard formulas

$$\langle \frac{1}{2} \mu_N | S_m | \frac{3}{2} \mu_{\Delta} \rangle = \sqrt{2} \langle \frac{3}{2} \mu_{\Delta} 1 m | \frac{1}{2} \mu_N \rangle \quad \text{and} \quad \langle \frac{1}{2} t_N | T_{\lambda} | \frac{3}{2} t_{\Delta} \rangle = \sqrt{2} \langle \frac{3}{2} t_{\Delta} 1 \lambda | \frac{1}{2} t_N \rangle. \quad (29)$$

Here the notations $\mu_{\Delta}(t_{\Delta})$ and $\mu_N(t_N)$ are used for the spin (isospin) projections of the initial Δ -isobar and the intermediate nucleon N as it is shown in the left-hand side of the diagram in Fig. 10.

The self energy (27) modifies the bare mass $M_{\Delta}^0(3q)$ of the three-quark shell-model Δ -isobar state

$$M_R(E) = M_{\Delta}^0(3q) + \mathcal{R}e \Sigma_{\Delta}(E) \quad (30)$$

and the imaginary part of $\Sigma_{\Delta}(E)$ defines the Δ -isobar width

$$\Gamma_R(E) = -2 \mathcal{I}m \Sigma_{\Delta}(E) \quad (31)$$

Due to the self-energy part of the mass operator the free Δ -isobar Green function $G_{\Delta}^0(E) = (E - M_{\Delta}^0(3q))^{-1}$ transforms into the (non-relativistic) propagator of a non-stable particle

$$G_R(E) = \left(E - M_R(E) + \frac{i}{2} \Gamma_R(E) \right)^{-1} \quad (32)$$

and the following on-mass-shell condition should be satisfied:

$$\begin{cases} M_R(E=M_{\Delta}) = M_{\Delta} & \text{at } M_{\Delta}=1232 \text{ MeV,} \\ \Gamma_R(E=M_{\Delta}) = \Gamma_{\Delta} & \text{at } \Gamma_{\Delta}=120 \text{ MeV.} \end{cases} \quad (33)$$

The $\pi N \Delta$ vertex function Eq.(28) predicts the value of the vertex constant $f_{\pi N \Delta}^0$ and Eq. (28) relates the vertex form factor $F_{\pi N \Delta}^0(k^2)$ to the momentum distribution of quarks in the nucleon

$$f_{\pi N \Delta}^0 = 2\sqrt{2} f_{\pi qq} \quad \text{and} \quad F_{\pi N \Delta}^0(k^2) \equiv F_{QM}^0(k^2) = e^{-k^2 b^2/6} \quad (34)$$

We consider the function $F_{QM}^0(k^2)$ as a quark-motivated vertex form factor and apply Eq.(16) for modification of all the meson-baryon and photon-baryon vertices.

TABLE I: Pion decay widths of baryon resonances in the 3P_0 model.

		B			
		$N(940)$	$\Delta(1232)$	$R(1440)$	$N^*(1535)$
3P_0 model	$f_{\pi NB}/f_{\pi NN}$	1	$\frac{3}{5}2\sqrt{2}$	$\frac{3}{5}\frac{5\alpha}{\sqrt{3}}$	$\frac{3}{5}\frac{2\sqrt{2}\beta}{\sqrt{3}}$
	$\Gamma(\text{MeV})$		64	47	52
Realistic model	$\Gamma_R(\text{MeV})$		120	88	98
exp.	$\Gamma_B(\text{MeV})$		120	210-245	52-83

In this simple model the decay widths Γ of the lowest nucleon excitations $B = \Delta, R, N^*$ into the pion channel ($B \rightarrow \pi + N$) amount to 50-60% of the experimental ones. The Γ calculated at $b_\pi/b = 0.5$ in the 3P_0 model are listed in Table I. The Δ -isobar width Γ_Δ does not depend on the pion radius b_π , but for orbital or radial excitations (N^*, R) such a dependence is important. The value $b_\pi/b \approx 0.5$ leads to an optimal value of the width of each resonance.

In a more realistic model the FSI in the decay channel $N + \pi$ should be taken into account, e.g. in terms of the unitary transformation method [30]. As it was shown by Ref. [30] the final result obtained by taking into account the full non-resonance interaction in the πN channel is equivalent to a small renormalization of the ‘‘bare’’ $\pi N \Delta$ coupling constant Eq.(34):

$$f_{\pi N \Delta}^0 \rightarrow f_{\pi N \Delta} = Z_R f_{\pi N \Delta}^0, \quad (35)$$

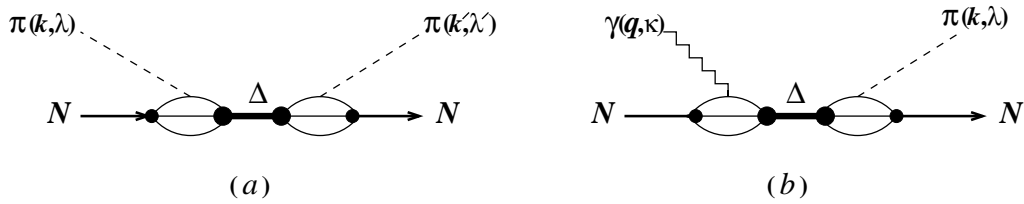
with $Z_R \approx 1.3$. Following this prescription we obtain a very similar result using the quark motivated form factor F_{QM} , namely $Z_R = 1.37$. The substitution of Eq. (35) in Eqs. (27) and (28) does not violate the unitarity of final results. Thus in practice, the usage of this prescription is more convenient than the summation of many Born terms in the πN FSI. The renormalized values of the decay widths Γ_R of the lowest baryon resonances are shown in Table I in comparison with the experimental ones Γ_B .

The results in Table I were obtained with the following values of parameters α, β and x determined in the 3P_0 -model:

$$\alpha = 3a + \frac{m_\pi}{m_q} \left(1 - \frac{a}{3} + \frac{5a^2}{9}\right), \quad \beta = \frac{m_\pi}{m_q b} \left(1 - \frac{2a}{3}\right), \quad a = x^2(1 + 2x^2/3)^{-1} \quad \text{and} \quad x = b_\pi/b = 0.5. \quad (36)$$

The widths Γ and Γ_R are calculated with the standard values for the coupling constants $f_{\pi qq} = \frac{3}{5}f_{\pi NN}$ and $f_{\pi NN} = 1$, and for the scale parameter and $b = 0.6$ fm.

The contribution of a virtual Δ -isobar to pion-production processes is described by the following amplitudes (Fig. 11):

FIG. 11: Resonance Δ -isobar contributions to physical processes.

(a) the πN resonance scattering sketched in Fig. 11(a) is written as

$$\frac{v_\Delta(\mathbf{k}', \lambda') v_\Delta^\dagger(\mathbf{k}, \lambda)}{E - M_R(E) + \frac{i}{2}\Gamma_R(E)}, \quad (37)$$

(b) the pion photo-production through an intermediate Δ -isobar of Fig. 11(b)

$$\frac{v_\Delta(\mathbf{k}, \lambda) w_\Delta^\dagger(\mathbf{q}, \kappa)}{E - M_R(E) + \frac{i}{2}\Gamma_R(E)}, \quad (38)$$

where the e.-m. vertex $w_{\Delta}^{\dagger}(\mathbf{q}, \varkappa)$ for the M1 transition $N + \gamma \rightarrow \Delta$

$$w_{\Delta}^{\dagger}(\mathbf{q}, \varkappa) = 3\langle N | H_{\gamma qq}^{(3)}(\mathbf{q}, \varkappa) | \Delta \rangle = -i \left(\frac{\sqrt{2}e}{2m_q} \right) e^{-q^2 b^2 / 6} [\mathbf{S}^{\dagger} \times \mathbf{q}] \cdot \boldsymbol{\epsilon}^{(\varkappa)} T_z \quad (39)$$

is calculated with the elementary quark-photon coupling operator

$$H_{\gamma qq}^{(3)}(\mathbf{q}, \varkappa) = \frac{e^{(3)}}{2m_q} e^{-i\frac{2}{3}\mathbf{q}\cdot\boldsymbol{\rho}} \boldsymbol{\epsilon}^{(\varkappa)} \cdot \left(-2i\nabla_{\rho} + 2\mathbf{q}/3 - i[\boldsymbol{\sigma}^{(3)} \times \mathbf{q}] \right), \quad (40)$$

where $e^{(3)} = 1/6 + \tau_z^{(3)}/2$.

B. Testing the model in pion photoproduction off the nucleon

The gauge invariance and the current conservation constraint has been actively used to define additional contributions to the photoproduction amplitude in the Δ -resonance region. The most important ones are the nucleon-pole and pion-in-flight diagrams with the seagull term added for the current conservation (see Fig. 12).

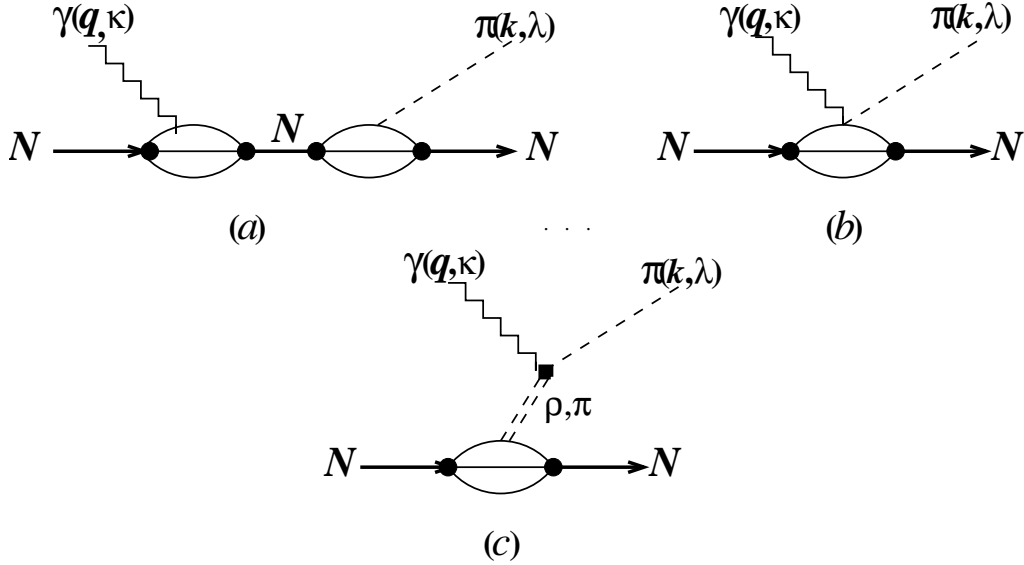


FIG. 12: Non-resonance contributions to the pion photoproduction amplitude.

All the terms have been evaluated in the above quark approach. The nucleon pole term depicted in Fig. 12(a) has the form analogous to the pole term in Eq. (38)

$$\frac{v_N(\mathbf{k}, \lambda) w_N^{\dagger}(\mathbf{q}, \varkappa)}{E - M_N}, \quad (41)$$

with

$$v_N(\mathbf{k}, \lambda) = 3\langle N(\mu', t') | H_{\pi qq}^{(3)}(\mathbf{k}, \lambda) | N(\mu_P, t_P) \rangle = i \left(\frac{5f_{\pi qq}}{3m_{\pi}} \right) e^{-k^2 b^2 / 6} \langle \mu' | \boldsymbol{\sigma} \cdot \mathbf{k} | \mu_P \rangle \langle t' | \tau_{\lambda} | t_P \rangle, \quad (42)$$

and

$$w_N^{\dagger}(\mathbf{q}, \varkappa) = 3\langle N(\mu_P, t_P) | H_{\gamma qq}^{(3)}(\mathbf{q}, \varkappa) | N(\mu, t) \rangle = -i \left(\frac{e}{2m_q} \right) e^{-q^2 b^2 / 6} \langle \mu_P | [\boldsymbol{\sigma}^{\dagger} \times \mathbf{q}] \cdot \boldsymbol{\epsilon}^{(\varkappa)} | \mu \rangle \langle t_P | \tau_z | t \rangle \quad (43)$$

The contact (“seagull”) term of Fig. 12(b) is calculated as matrix element

$$\mathcal{M}_{sea}(\mathbf{q}, \varkappa; \mathbf{k}, \lambda) = 3\langle N | H_{sea}^{(3)}(\mathbf{q}, \varkappa; \mathbf{k}, \lambda) | N \rangle \quad (44)$$

of the operator

$$H_{sea}^{(3)}(\mathbf{q}, \boldsymbol{x}; \mathbf{k}, \lambda) = i\lambda e^{\frac{f_{\pi qq}}{m_\pi} \tau_{-\lambda}^{(3)} \boldsymbol{\sigma}^{(3)} \cdot \boldsymbol{\epsilon}^{(\boldsymbol{x})}} e^{2i(\mathbf{k}-\mathbf{q}) \cdot \boldsymbol{\rho}/3} \quad (45)$$

obtained by ‘‘gauging’’ of the PV πqq interaction Lagrangian $\mathcal{L}_{\pi qq}^{PV} = \frac{f_{\pi qq}}{m_q} \bar{\psi}_q \gamma^\mu \gamma_5 \boldsymbol{\tau} \psi_q \cdot \partial_\mu \boldsymbol{\varphi}$. The expression for the operator is taken in Eq. (45) in a non-relativistic limit. The final expression for the matrix element of Eq.(44) can be written in the form of a series:

$$\mathcal{M}_{sea}(\mathbf{q}, \boldsymbol{x}; \mathbf{k}, \lambda) = -ie \lambda \tau_{-\lambda} \boldsymbol{\sigma} \cdot \boldsymbol{\epsilon}^{(\boldsymbol{x})} \left(\frac{5f_{\pi qq}}{3m_\pi} \right) e^{-k^2 b^2/6} e^{-q^2 b^2/6} \times [i_0(kqb^2/3) + 3\hat{\mathbf{k}} \cdot \hat{\mathbf{q}} i_1(kqb^2/3) + \dots],$$

The pion-in-flight diagram is shown in Fig. 12(c). Its contribution takes the form:

$$\mathcal{M}_{\pi\pi}(\mathbf{q}, \boldsymbol{x}; \mathbf{k}, \lambda) = ie \lambda \tau_{-\lambda} \left(\frac{5f_{\pi qq}}{3m_\pi} \right) \mathbf{k} \cdot \boldsymbol{\epsilon}^{(\boldsymbol{x})} \frac{\boldsymbol{\sigma} \cdot (\mathbf{q} - \mathbf{k})}{2(\omega_\pi q_0 - \mathbf{k} \cdot \mathbf{q})} e^{-k^2 b^2/6} e^{-q^2 b^2/6} \times [i_0(kqb^2/3) + 3\hat{\mathbf{k}} \cdot \hat{\mathbf{q}} i_1(kqb^2/3) + \dots], \quad (46)$$

The Δ -isobar and nucleon pole terms in Eqs.(38) and (Eq.41) imply the summation over spin and isospin projections of the intermediate Δ or N (μ_Δ, t_Δ or μ_P, t_P correspondingly), and thus the full expressions for these terms are

$$\begin{aligned} \mathcal{M}_{\Delta\pi}(\mathbf{q}, \boldsymbol{x}; \mathbf{k}, \lambda) &= - \left(\frac{2\sqrt{2}f_{\pi qq}}{m_\pi} \right) \left(\frac{\sqrt{2}e}{2m_q} \right) \frac{e^{-k^2 b^2/6} e^{-q^2 b^2/6}}{\sqrt{s} - M_R(s) + \frac{i}{2}\Gamma_\Delta(s)} \\ &\times \sum_{\mu_\Delta} \langle \mu' | \mathbf{S} \cdot \mathbf{k} | \mu_\Delta \rangle \langle \mu_\Delta | \boldsymbol{\epsilon}^{(\boldsymbol{x})} \cdot [\mathbf{S}^\dagger \times \mathbf{q}] | \mu \rangle \sum_{t_\Delta} \langle t' | T_{-\lambda} | t_\Delta \rangle \langle t_\Delta | T_z^\dagger | t \rangle \end{aligned} \quad (47)$$

and

$$\begin{aligned} \mathcal{M}_{N\pi}(\mathbf{q}, \boldsymbol{x}; \mathbf{k}, \lambda) &= - \left(\frac{5f_{\pi qq}}{3m_\pi} \right) \left[\frac{1}{6} + (-1)^{t-1/2} \frac{5}{6} \right] \left(\frac{e}{2m_q} \right) \frac{e^{-k^2 b^2/6} e^{-q^2 b^2/6}}{\sqrt{s} - M_N} \\ &\times \sum_{\mu_P} \langle \mu' | \boldsymbol{\sigma} \cdot \mathbf{k} | \mu_P \rangle \langle \mu_P | \boldsymbol{\epsilon}^{(\boldsymbol{x})} \cdot [\boldsymbol{\sigma} \times \mathbf{q}] | \mu \rangle \sum_{t_P} \langle t' | \tau_{-\lambda} | t_P \rangle \langle t_P | \tau_z | t \rangle \end{aligned} \quad (48)$$

The numerical results on the energy dependence of the π^0 and π^- photoproduction cross sections are shown in Fig. 13 in comparison with the conventional model results in which the phenomenological πN -coupling constants and form factors are used for the same hadron vertices as shown in Figs. 11 and 12. One can see a good agreement between results of both models and the data. For the charged pion π^- the contributions of two main terms, the Δ -resonance and seagull, are shown separately in Fig. 13 on the right panel.

For the reaction $\gamma p \rightarrow \pi^0 p$ the differential cross section are shown in Fig. 14 for photon energies of $E_\gamma=300$ and 350 MeV, while the for the $\gamma n \rightarrow \pi^- p$ reaction energies of $E_\gamma=194$ and 270 MeV have been selected (Fig. 15).

The CQM is seen to lead to reasonable results for pion photoproduction off the nucleon, and thus this model can be employed to describe similar processes off the deuteron, where one can expect this model to predict new effects related to the $N\Delta$ FSI at short ranges.

IV. PION PHOTOPRODUCTION OFF THE DEUTERON

The quark model calculations of cross sections for pion photoproduction off the deuteron in the Δ resonance region have been performed in the framework of the Moscow-Tübingen model for NN interaction. The results are similar to the conventional model results without $N\Delta$ FSI. But taking into consideration the short-range $N\Delta$ FSI leads to an additional effect of suppression of the forward-angle π^0 photoproduction similar to the suppression obtained in Ref. [21] due to the NN FSI.

The expressions for the loop diagrams of Figs. 8a) and 9 are illustrated by the expanded diagrams in Fig. 16 for better visualization of the main blocks of the expressions.

Our calculation of the π^0 photoproduction (Fig. 16, left) use a loop integral which can be expressed in the form:

$$\begin{aligned} \mathcal{M}_{d\gamma \rightarrow \pi^0 np}(\mathbf{q}, \boldsymbol{x}; \mathbf{k}, \lambda; \mathbf{p}') &= \int \frac{d^3 p}{(2\pi)^3} \Psi_d(\mathbf{p}) w_\Delta(\mathbf{q}, \boldsymbol{x}) \frac{g_0 \varphi_{2s}(\mathbf{p} + \mathbf{q}/2)}{W_\Delta(\mathbf{p}) - M_R(W_\Delta(\mathbf{p})) + \frac{i}{2}\Gamma_R(W_\Delta(\mathbf{p}))} \\ &\times I_0(s^{1/2}) \frac{g_0 \varphi_{2s}(\mathbf{p}' + \mathbf{k}/2)}{W'_\Delta(\mathbf{p}') - M_R(W'_\Delta(\mathbf{p}')) + \frac{i}{2}\Gamma_R(W'_\Delta(\mathbf{p}'))} v_\Delta(\mathbf{k}, \lambda), \end{aligned} \quad (49)$$

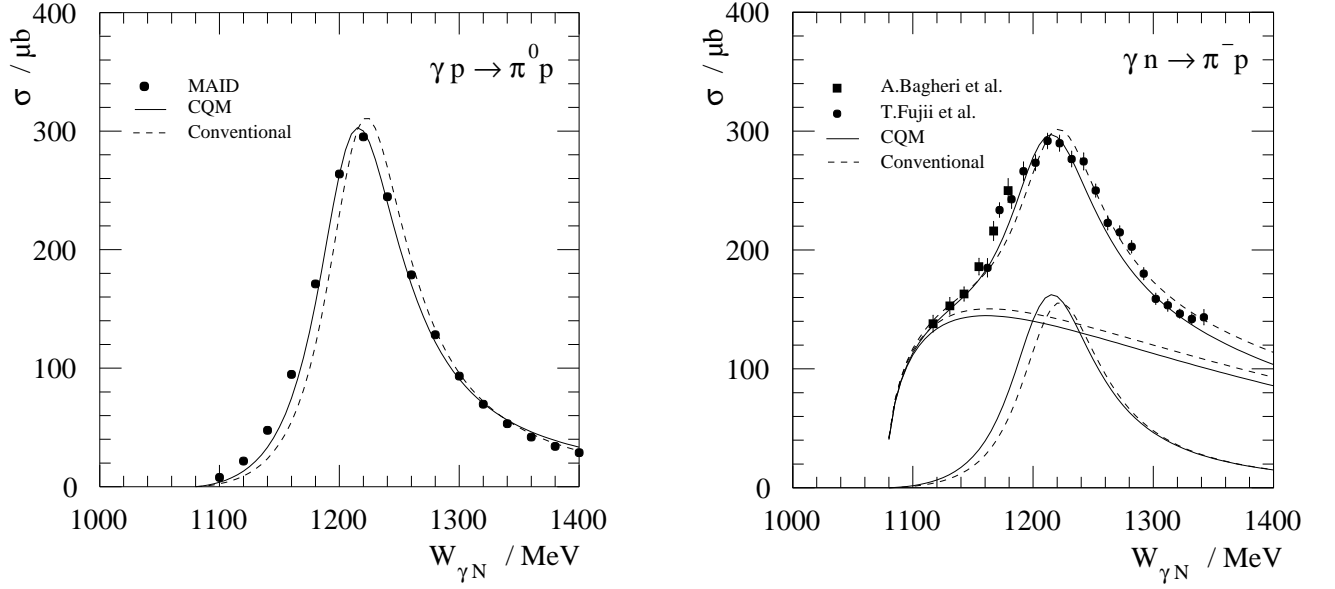


FIG. 13: Total cross section for π^0 photoproduction off the proton (left) and for π^- photoproduction off the neutron (right). Calculations in conventional (dash line) and quark (solid line) models. The data are taken from Refs. [33] for π^0 and [31] for π^- , respectively.

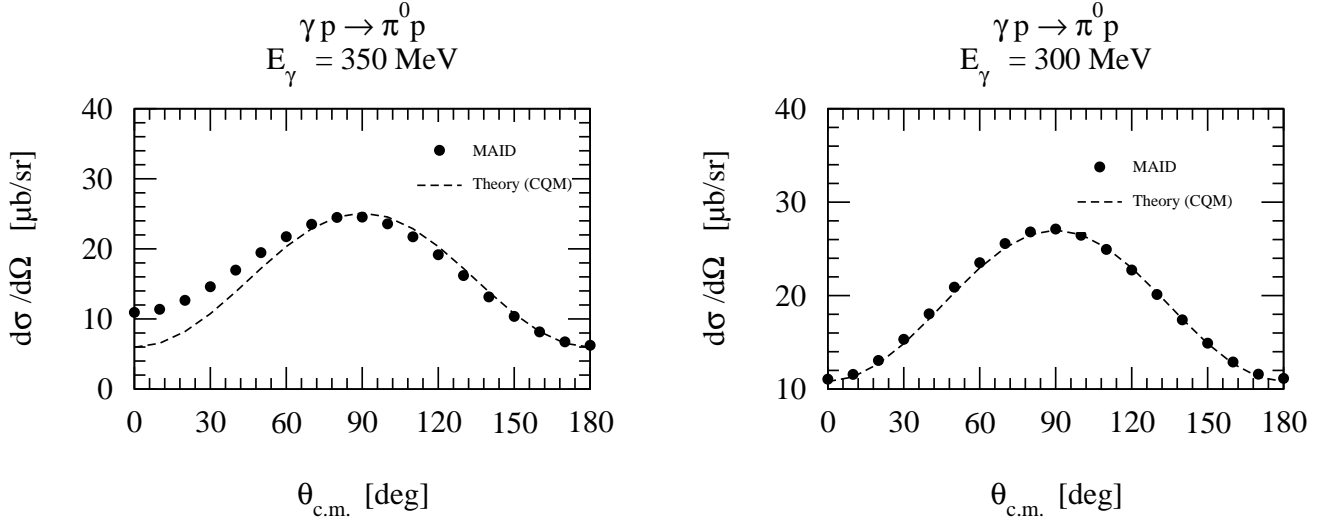


FIG. 14: Differential cross section for π^0 photoproduction in comparison to the data from Refs. [31, 33]

for $\lambda=0$, where $s^{1/2} = \sqrt{M_d(M_d + 2E_\gamma)} \approx M_d + E_\gamma$ is the mass of the initial $\gamma + d$ state. The energies of the off-shell Δ in the loop (W_Δ) and in the final $N\Delta$ state (W'_Δ) are given by the expressions

$$\begin{aligned}
 W_\Delta(\mathbf{p}) &\equiv s_\Delta^{1/2}(\mathbf{p}), & s_\Delta(\mathbf{p}) &= (M_d - E_p + E_\gamma)^2 - (\mathbf{p} + \mathbf{q})^2, \\
 W'_\Delta(\mathbf{p}') &\equiv s_\Delta^{1/2}(\mathbf{p}'), & s_\Delta(\mathbf{p}') &= (M_N + \omega_\pi)^2 + 2\omega_\pi(E'_p - M_N), \\
 E_p &= \sqrt{M_N^2 + \mathbf{p}^2} & \text{and } E'_p &= \sqrt{M_N^2 + (\mathbf{p}' + (\mathbf{q} - \mathbf{k})/2)^2}.
 \end{aligned} \tag{50}$$

They depend on relative momenta of nucleons in the deuteron $\mathbf{p} = (\mathbf{p}_1 - \mathbf{p}_2)/2$ and in the final state $\mathbf{p}' = (\mathbf{p}'_1 - \mathbf{p}'_2)/2$ respectively (see the momentum designations in Fig. 16). Note that the above expression for the energy E_p of the second nucleon (with momentum $\mathbf{p}_2 = -\mathbf{p}$) implies that the nucleon-spectator is proposed to be on its mass shell.

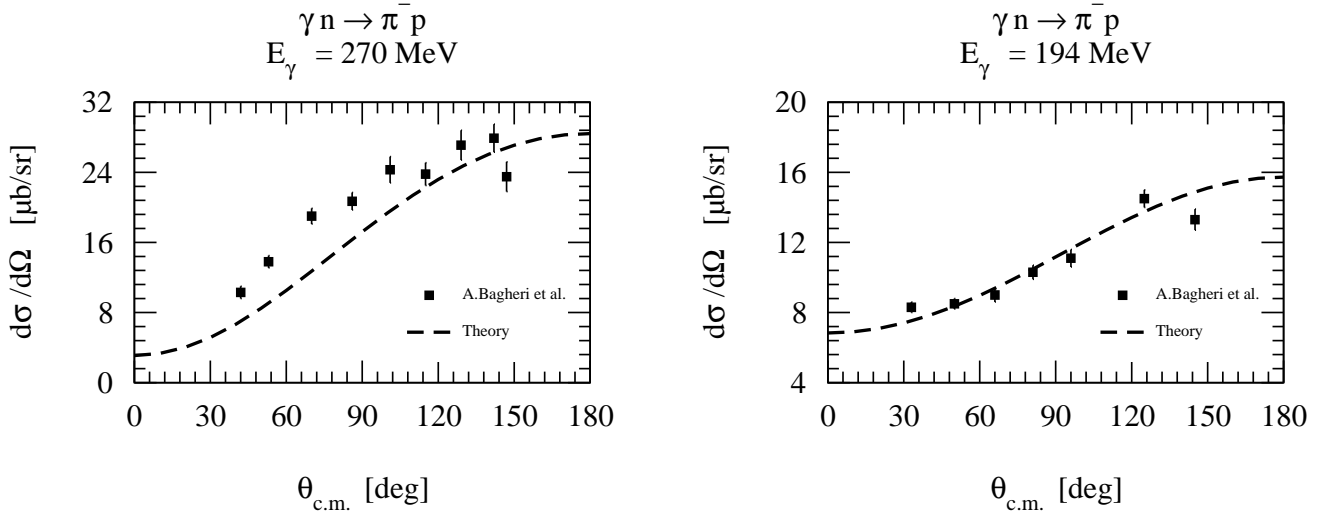


FIG. 15: Differential cross section for π^- photoproduction in comparison to the data from Ref. [32].

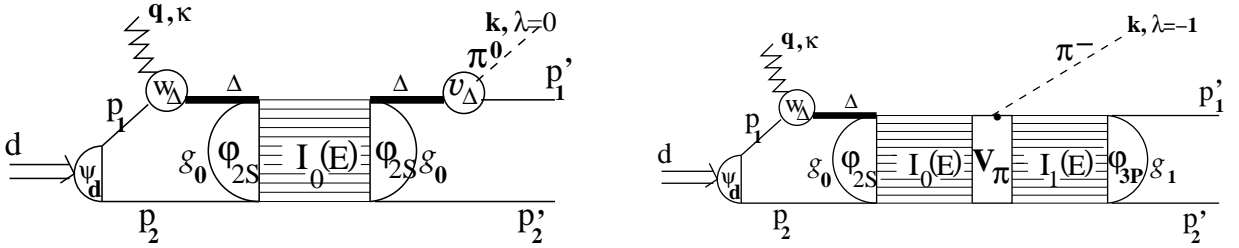


FIG. 16: The dressed-bag model. The main blocks of the loop diagrams of $N\Delta$ FSI for π^0 (left) and π^- (right) photoproduction.

For the π^- photoproduction the loop integral for the right diagram in Fig. 16 is expressed in a similar form

$$\begin{aligned} \mathcal{M}_{d\gamma \rightarrow \pi^- np}(\mathbf{q}, \varkappa; \mathbf{k}, \lambda; \mathbf{p}') = & \int \frac{d^3p}{(2\pi)^3} \Psi_d(\mathbf{p}) w_\Delta(\mathbf{q}, \varkappa) \frac{g_0 \varphi_{2S}(\mathbf{p} + \mathbf{q}/2)}{W_\Delta(\mathbf{p}) - M_R(W_\Delta(\mathbf{p})) + \frac{i}{2}\Gamma_R(W_\Delta(\mathbf{p}))} \\ & \times I_0(s^{1/2}) V_\pi(k, \lambda) I_1(s^{1/2}) g_1 \varphi_{3P}(\mathbf{p}'), \quad \text{for } \lambda = -1, \end{aligned} \quad (51)$$

with an additional dressed-bag transition vertex $V_\pi(k, \lambda)$ instead of the $\pi N\Delta$ vertex $v_\Delta(\mathbf{k}, \lambda)$, where the matrix element

$$V_\pi(k, \lambda = -1) = - \left(\frac{44\sqrt{2}f_{\pi qq}}{45m_\pi b} \right) \left(\frac{\omega_\pi}{2m_q} + \frac{k^2 b^2}{6} \right) e^{k^2 b^2/6} \quad (52)$$

for the transition $D_0(s^6) \rightarrow d_1(s^5 p) + \pi(l_\pi=0)$ has been as usually taken from the 3P_0 model in the limit (Eq.9).

In Eqs. (49) and (51) the vertex constants g_0 and g_1 are the algebraic values from Eq. (15) from S - and P -wave $N\Delta$ and NN channels, respectively. Similarly, the pole factors $I_0(s^{1/2})$ and $I_1(s^{1/2})$ are functions (21) with parameters given by Eq.(22). The S -wave deuteron wave function $\Psi_d(\mathbf{p})$ in the loop integrals [Eqs.(49) and (51)] has been taken from the dressed-bag model [11] directly. The $\pi N\Delta$ and $\gamma N\Delta$ vertices $v_\Delta(\mathbf{k}, \lambda)$ and $w_\Delta(\mathbf{q}, \varkappa)$ in the integrand of Eqs. (49) and (51) are defined in Eqs. (28) and (Eq.39) (see also renormalization conditions in (Eq.16) and (Eq.35)). The summation over spin and isospin projections μ, μ', t and t' of nucleons and Δ s with Clebsch-Gordan coefficients in Eqs. (49) and (51) is omitted here to simplify reading.

The results of the calculations with and without $N\Delta$ FSI for the $\gamma d \rightarrow \pi^0 np$ are shown in Fig. 17 for the differential cross sections taken at three photon energies. Results for two variants of FSI are shown: the dash-dot curve corresponds to the value of effective coupling constant $g_{\Delta\sigma q}$ obtained by renormalization of the NN parameters (22) with the algebraic factors C_{ST}^Δ/C_{ST}^N of Eq. (15), while the solid curve corresponds to the non-renormalized values of the parameters (22). From these two curves it is possible to make rough estimates of model dependence of the results.

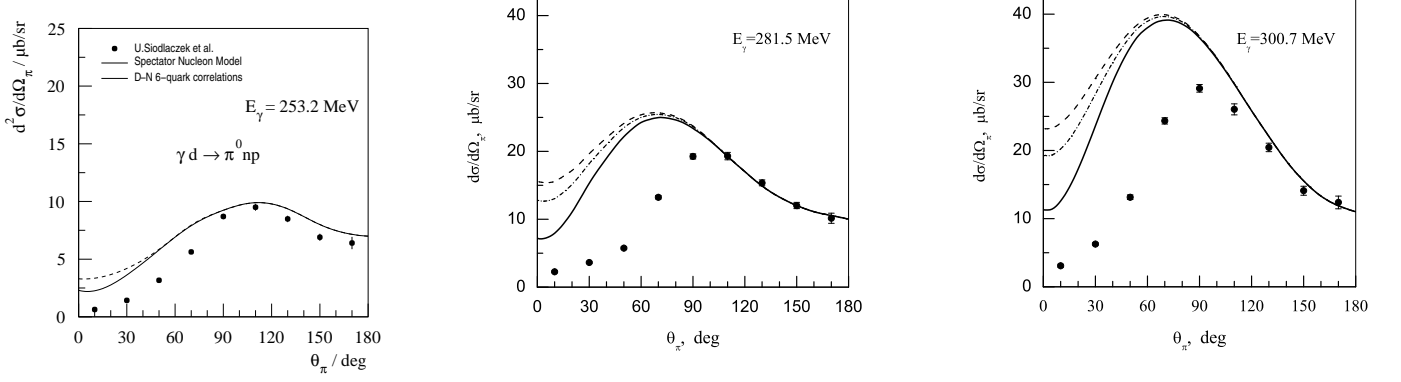


FIG. 17: The differential cross sections for π^0 photoproduction off the deuteron [34] taken at 3 photon energies (E_γ is in the c.m. of $\gamma - d$ system) compared to the quark model predictions. Results for the quasi-free mechanism of photoproduction are shown by the dashed line, while the combined effect of the quasi-free mechanism and the Born diagram of the $N\Delta$ FSI is shown by the dash-dot and solid lines (for the renormalized value of the coupling constant $g_{\Delta\sigma q}$ from Eq. (15) and for the non-renormalized value $g_{\Delta\sigma q} = g_{N\sigma q}$ respectively).

The total cross sections for the $\pi^0 np$ and the $\pi^- pp$ channels are compared in Fig. 18. One can see that including the $N\Delta$ FSI in terms of the six-quark bag diagram of Fig. 8(a) leads to a detectable effect for both the differential and integral cross sections of π^0 production. It is also seen that the contribution of the $N\Delta$ FSI to the π^0 photoproduction has a resonance character, and out of the resonance region (e.g. at $E_\gamma = 253.2$ MeV in the c.m. of $\gamma - d$ system) the contribution becomes a negligibly small quantity.

Still, a discrepancy to the data remains. However, for the π^- photoproduction (Fig. 18) the FSI is not so important as for the π^0 . These results are consistent with our qualitative consideration in Sect.II D.

V. CONCLUSIONS

The dressed-bag model predictions for the contribution of $N\Delta$ FSI to the $d(\gamma, \pi^0)np$ and $d(\gamma, \pi^-)pp$ cross sections are qualitatively consistent with the data, but full calculations with the off-shell amplitudes of NN and $N\Delta$ FSI are

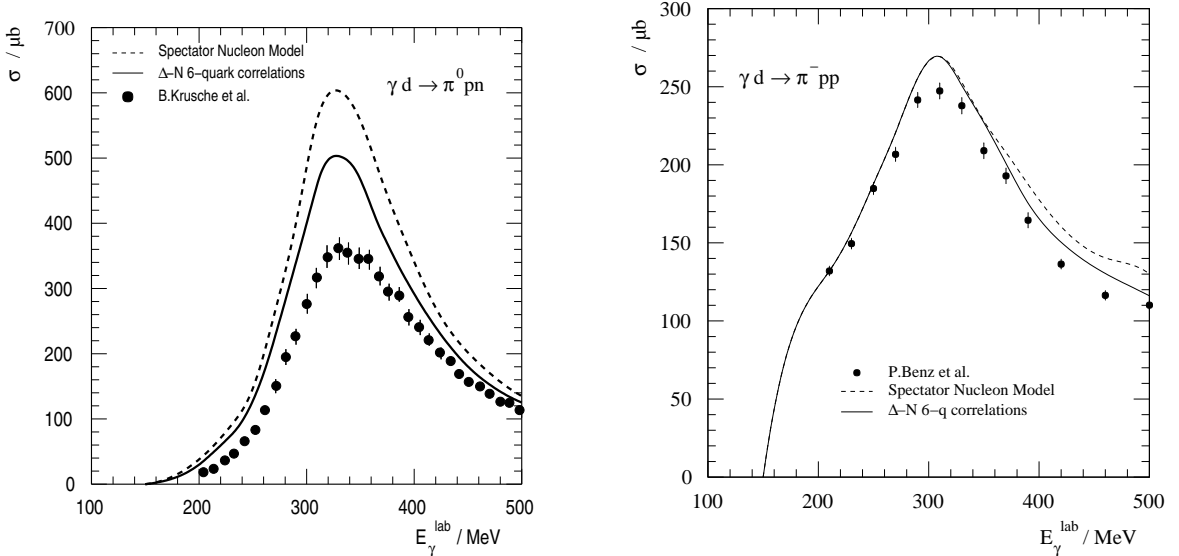


FIG. 18: Left: The total cross sections for π^0 photoproduction off the deuteron [22] in comparison to those calculated in the quark model (full lines). Right: Total cross section of π^- photoproduction. Data are from Ref. [32].

necessary to obtain a quantitative description of the cross sections.

It is well known [21] that the main correction to the quasi-elastic (spectator) mechanism of π^0 photoproduction off the deuteron is due to $n-p$ rescattering in the final state (diagrams in Fig. 1b). The present calculation demonstrates that the cross section of the reaction $\gamma d \rightarrow \pi^0 np$ is also sensitive to the final-state $N\Delta$ interaction at least in the Δ -resonance region for forward pion angles.

Our results can only be considered as a first step towards a quantitative description of photoproduction processes with taking into account both quark and meson degrees of freedom. Now we can only state some qualitative implications of the study:

- i) It is shown that the CQM (supplemented by a simple dressing procedure based on the 3P_0 model) not only leads to a workable approach to the pion photoproduction off the nucleon, but it can also be used for evaluations of photoproduction cross sections on lightest nuclei, e.g. D and ^3He .
- ii) The dressed-bag model of short-range NN and $N\Delta$ interaction based on an analysis of the configuration mixing in the overlap region predicts a destructive interference of the $N\Delta$ FSI loop diagram (Fig. 8a) with the quasi-elastic photoproduction Born amplitudes calculated within the CQM.
- iii) This model predicts new types of NN and $N\Delta$ short-range correlations that would be desirable to investigate in photoproduction reactions on lightest nuclei, e.g. in polarization experiments as it was proposed in Sect. II D for the mechanism shown in Fig. 9 (another polarization experiments was recently proposed in Ref. [35]).

The most important conclusion which can be derived from the above CQM consideration is that the short-range baryon-baryon interaction is determined by a bag-like six-quark state. Despite the fact that the bag has its own meson cloud this short-range interaction has a non-Yukawa form and directly leads to the s -channel singularity of amplitudes. In experiments at more high energies $E_\gamma \gtrsim 1-2$ GeV, where the t -channel singularities become extinct because of form factors, the s -channel singularities should lead to more pronounced contributions to observable effects.

VI. ACKNOWLEDGMENT

We gratefully acknowledge very useful discussions with Profs. V. Neudatchin, M. Rosina, B. Golli and Fl. Stancu and with Drs. V. Lyubovitskij, A. Machavariani and V.N. Pomerantsev. This work was supported by funds from the Russian Foundation for Basic Research (grants 01-02-04015 and 02-02-16612) and the Deutsche Forschungsgemeinschaft (Fa67/20-1, GRK683, Gr1084/3, and He2171/1).

-
- [1] D.A. Liberman, Phys. Rev. **D 16**, 1542 (1977); C.E. DeTar, Phys. Rev. **D 17**, 302 (1978).
 - [2] I.T. Obukhovskiy, V.G. Neudatchin, Yu.F. Smirnov and Yu.M. Tchuvil'skiy, Phys. Lett. **B88**, 231 (1979).
 - [3] M. Harvey, Nucl. Phys. **A352**, 301 (1981); 326 (1981).
 - [4] M. Cvetič, B. Golli, N. Mankoč-Borštnik and M. Rosina, Nucl. Phys. **A395**, 349 (1983).
 - [5] M. Oka and K. Yazaki, Prog. Theor. Phys. **66**, 556 (1981); 572 (1981).
 - [6] A. Faessler, F. Fernandez, G. Lübeck and Shimizu, Nucl. Phys. **A402**, 555 (1983).
 - [7] D. Bartz and Fl. Stancu, Phys. Rev. **C63**, 034001 (2001).
 - [8] Yu.A. Simonov, Sov. J. Nucl. Phys. **36**, 422 (1982); **38**, 939 (1983).
 - [9] B.L.G. Bakker and I.M. Narodetskiy, Advances in Nucl. Phys. **21**, 1 (1994).
 - [10] L.S. Kisslinger, Phys. Lett. **B112**, 1307 (1982); T.S. Cheng and L.S. Kisslinger, Phys. Rev. **C35**, 1432 (1987).
 - [11] V.I. Kukulin, I.T. Obukhovskiy, V.N. Pomerantsev and Amand Faessler, Int. J. Mod. Phys. **E11**, 1 (2002); J. Phys. G: Nucl. Part. Phys. **27**, 1851 (2001).
 - [12] A.M. Kusainov, V.G. Neudatchin and I.T. Obukhovskiy, Phys. Rev. **C44**, 2343 (1991); I.T. Obukhovskiy, Prog. Part. Nucl. Phys. **36**, 359 (1996).
 - [13] A.W. Thomas, Adv. Nucl. Phys. **13**, 1 (1984).
 - [14] M.M. Giannini, Rep. Prog. Phys. **54**, 453 (1991); D. Drechsel and M. Vanderhaeghen, Phys. Rev. **C64**, 065202 (2001).
 - [15] A. Le Yaouanc, L. Oliver, O. Pène and J.-C. Raynal, *Hadron Transitions in the Quark Model*, (Gordon and Breach Science Publishers, N.-Y., 1988).
 - [16] D.O. Riska and G.E. Brown, Nucl. Phys. **A679**, 577 (2001); L.Ya. Glozman and D.O. Riska, Phys. Rep. **268**, 263 (1996).
 - [17] J.M. Laget, Phys. Rep. **69**, 1 (1981).
 - [18] R. Schmidt, H. Arenhövel and P. Wilhelm, Z. Phys. **A355**, 421 (1996).
 - [19] M.I. Levchuk, V.A. Petrun'kin and M. Schumacher, Z. Phys. **A355**, 317 (1996).
 - [20] V. Kolybasov and V. Ksenzov, Sov. J. Nucl. Phys. **22**, 372 (1976).
 - [21] M.I. Levchuk, M. Schumacher, and F. Wissman, Nucl. Phys. **A675**, 621 (2000).

- [22] B. Krusche *et al.*, Eur. Phys. J. **A6**, 309 (1999).
- [23] P. Sauer, Prog. Part. Nucl. Phys. **16**, 35 (1986).
- [24] H. Feshbach, Ann. Phys. (N.Y.) **5**, 357 (1958); **19**, 287 (1962).
- [25] I.T. Obukhovskiy, A. Faessler, G. Wagner and A.J. Buchmann, Phys. Rev. **C60**, 035207 (1999).
- [26] F. Cano, P. González, S. Noguera and B. Deplanques, Nucl. Phys. **A603**, 257 (1996).
- [27] C. Schütz, J. Heidenbauer and J. Speth, Phys. Rev. **C57**, 1464 (1998).
- [28] T. Gutsche, R.D. Viollier and A. Faessler, Phys. Lett. **B331**, 8 (1994).
- [29] L. Heller, S. Kumano, J.C. Martinez, Phys.Rev. **C35**, 718 (1987).
- [30] T. Sato and T.-S.H. Lee, Phys.Rev. **C54**, 2660 (1996).
- [31] A. Bagheri *et al.*, Phys.Rev. **C38**, 875 (1988); T. Fujii et al., Nucl.Phys. **B120**, 395 (1977).
- [32] P. Benz *et al.*, Nucl.Phys. **B65**, 158 (1973).
- [33] MAID, L. Tiator, Mainz, <http://www.kph.uni-mainz.de/MAID>.
- [34] U. Siodlaczek *et al.*, Eur. Phys. J. **A10**, 365 (2001).
- [35] M.P. Rekalo, and E. Tomasi-Gustafson, arXiv: nucl-th/0111032.
- [36] The h.o. radius $b \approx 0.5-0.6$ fm of the non-relativistic quark model corresponds to the characteristic confinement scale of the QCD $\Lambda_{QCD} \approx 200$ MeV, but the high-momentum behaviour of F_{QM} in loop integrals should also depend on a higher characteristic scale $\Lambda_{ch} \approx 0.6-1$ GeV related to the spontaneous breaking of chiral symmetry.